Antioxidant and antimicrobial emulsions with amphiphilic olive extract, nanocellulose-stabilized thyme oil and common salts for active paper-based packaging

Roberto J. Aguado, Elena Saguer, Quim Tarrés, Núria Fiol, Marc Delgado-Aguilar [*]

LEPAMAP-PRODIS Research Group, University of Girona, C/ Maria Aurèlia Capmany, 61, 17003 Girona, Spain

ARTICLE INFO

ABSTRACT

Anionic cellulose nanofibers (CNFs) were used to stabilize emulsions that combined water-soluble (and oil-soluble), strongly antioxidant extracts with a water-immiscible, notably antimicrobial essential oil. Specifically, the radical scavenging activity was primarily provided by aqueous extracts from olive fruit (*Olea europaea* L.), while the antimicrobial effects owed eminently to thyme oil (*Thymus vulgaris* L.). The resulting emulsions were highly viscous at low shear rate (4.4 Pa·s) and displayed yield stress. The addition of edible salts decreased the yield stress, the apparent viscosity and the droplet size, to the detriment of stability at ionic strengths above 50 mM. Once characterized, the antioxidant and antimicrobial emulsions were applied on packaging-grade paper. Coated paper sheets inhibited the growth of *Listeria monocytogenes*, a common foodborne pathogen, and acted as antioxidant emitters. In this sense, the release to food simulants A (ethanol 10 vol%), B (acetic acid 3 wt%), and C (ethanol 20 vol%) was assessed. A 24-hour exposure of 0.01 m^2 of coated paper to 0.1 L of these hydrophilic simulants achieved inhibition levels of the 2,2-diphenyl-1-picrylhydrazyl radical (DPPH) in the 15–29 % range. All considered, the bioactive properties of thyme essential oil towards lipophilic food products can be complemented with the antioxidant activity of aqueous olive extracts towards hydrophilic systems, resulting in a versatile combination for active food packaging.

1. Introduction

The incorporation of antioxidant and antimicrobial compounds in food packaging materials is one of the most common strategies to extend the shelf life of food products [1,2]. Despite the broad spectrum of active substances and support materials to accomplish such thing, current trends and concerns indicate that not everything fits. To fulfill the demands for food safety, environmental protection, and compliance to increasingly exigent regulations, some requirements should be met.

Regarding the support material, the massified use of non-biodegradable plastics should be progressively left behind in benefit of more sustainable alternatives, including cellulose paper [3,4]. In this sense, the European Union (EU) has passed, along the last few years, the so-called Plastic Bags Directive [5], the Single-Use Plastics Directive [6], and the Directive on Packaging and Packaging Waste [7]. Similar efforts are being made all around the globe. The largest plastic producer in the

word, the People's Republic of China, passed in 2020 a law restricting "the production, sale, and use of non-degradable plastic bags and other disposable plastic products" [8].

When it comes to bioactive substances, all factors along their life cycle must be considered: their production, how they are infused into packaging materials, potential toxicity, to what extent they migrate to food, and whether they affect the recyclability or compostability of active packaging. For instance, the most common antimicrobial agent proposed for packaging paper in the techno-scientific literature is silver, usually as silver nanoparticles [9,10], but they remain under consideration by food safety authorities [11]. Alternatively, many proposals highlight vegetable-sourced essential oils and extracts [2,12,13].

A previous study of ours has presented nanocellulose-stabilized emulsions of thyme essential oil (TEO) in water [14]. Those Pickering emulsions had only three components: TEO, water, and cellulose nanofibers produced after a regioselective oxidation mediated by the

---

(2,2,6,6-tetramethylpiperidin-1-yl)oxyl radical (TEMPO). TEO-in-water emulsions inhibited the growth of at least three common foodborne pathogens [15]. On the other hand, the lipophilic character of TEO hindered their release to hydrophilic food simulants, which is why only simulant D1 was chosen for radical scavenging assays [16]. Then, by analyzing data on plant extracts [17,18] and attempting to select one based on antioxidant and/or antimicrobial activity, safety, potential sensory impact on taste, and availability in Southern Europe, water-soluble extracts from olive fruit (*Olea europea* L.) seemed to offer a solid alternative [19,20].

To overcome the limitations of the aforementioned article and following the recent trend on nanocellulose-stabilized emulsions of essential oils in water [13,21], this new study combines TEO and olive fruit extracts (OFE) to prepare strongly antioxidant and antimicrobial emulsions. While the nanocellulose-mediated stabilization of immiscible essential oils, such as those from cinnamon and clove [21,22], has been extensively studied, the incorporation of amphiphilic extracts offers an opportunity for innovation. Unlike in common antimicrobial emulsions, active properties are not restricted to one of the phases. The amphiphilicity of OFE ensures that it is present in significant proportion in both the aqueous region and the essential oil. Furthermore, aiming at compensating the high hydrophilic character of charged nanocellulose [23,24], the effects of adding edible salts (NaCl, KCl, sodium citrate) on rheology, partition of phenolic compounds between the oil phase and the aqueous phase, droplet polydispersity, and stability are assessed. Selected stable emulsions are then used to coat packaging paper sheets, to be characterized in terms of performance as passive packaging, as antibacterial material, and as antioxidant emitter.

2. Experimental

2.1. Materials

Sodium bromide (NaBr), sodium hypochlorite (NaClO), sodium hydroxide (NaOH), absolute ethanol, Folin-Ciocalteu reagent, sodium carbonate (Na_2CO_3), sodium chloride (NaCl), potassium chloride (KCl),

sodium citrate, and gallic acid were acquired from Scharlab (Sentmenat, Spain). TEMPO, TEO, Mueller-Hinton (MH) agar, PALCAM *Listeria*-selective agar, and 1,1-diphenyl-2-picrylhydrazyl radical (DPPH) were received from Sigma-Aldrich (Barcelona, Spain). The base packaging paper for coating experiments and the source of cellulose for TOCNFs were respectively testliner (175 g/m^2) and a bleached kraft eucalyptus pulp, both of industrial origin.

OFE, commercialized by the name Mediteanox® as food supplement, was purchased from Granatum Plus (Murcia, Spain). In order to discard poorly soluble compounds, 5.0 g of this product were suspended in 50 mL of distilled water at 23 °C and stirred for 15 min. The aqueous suspension was vacuum-filtered over a Whatman® qualitative filter paper (pore size: 20–25 μm), the solids were discarded, and the filtrate was labeled as "OFE solution".

Non-pathogenic strains of *Listeria monocytogenes* (CECT4031) and *Escherichia coli* (ATCC10536) were obtained from the Spanish Type Culture Collection (Science Park of University of Valencia, Paterna, Spain) and from the American Type Culture Collection (Manasas, VA, USA), respectively.

To ease understanding, the core steps of the methodology for producing, characterizing and applying TEO/OFE/nanocellulose emulsions have been simplified and schematized in Fig. 1.

2.2. Production of nanocellulose

First, the bleached pulp was suspended in distilled water at 1.5 wt% consistency and dispersed at 3000 rpm for 10 min in a pulp disintegrator (IDM, Gipuzkoa, Spain) that complies to the ISO standard 5263 [25]. TEMPO-mediated oxidation was carried out as described elsewhere [26]. Briefly, 16 mg of TEMPO, 100 mg of NaBr and 15 mmol of NaClO were added per gram of pulp dispersed in water (1 wt% consistency), on the basis of dry pulp weight. The pH was kept above 10 through the reaction by additions of aqueous NaOH (1 M). Oxidation took place at 23 °C and under mechanical agitation (*ca.* 500 rpm), until the pH ceased to drop. At this point, TEMPO-oxidized cellulose was filtered (pore size: 74 μm), washed with cold distilled water, and diluted to 1.2 wt%
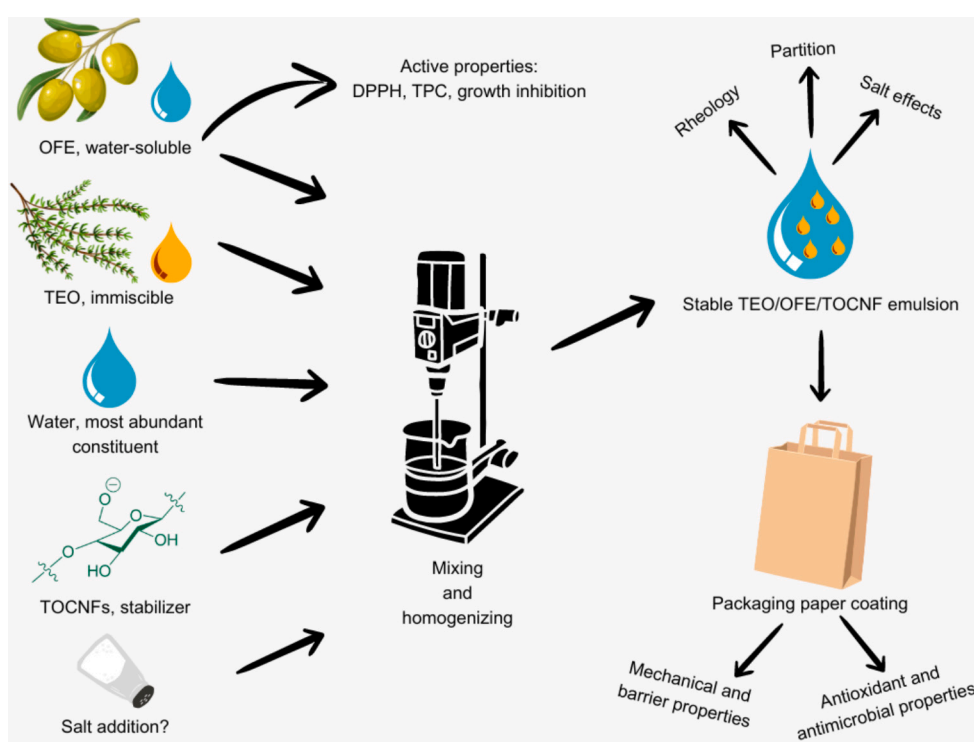

Fig. 1. Illustrated and simplify scheme of the experimental procedure.

consistency.

The slurry of TEMPO-oxidized cellulose was processed through a GEA Niro Soavi (Parma, Italy) Panda High Pressure Laboratory Homogenizer (HPS), model NS1001L2K. It was subjected to 3 passes at 300 bar, 3 passes at 600 bar, and 3 passes at 900 bar. The TOCNFs produced this way, once characterized as described elsewhere [26], contained 1.5 $\pm$ 0.1 mmol –COO$^-$/g. They had a cationic demand of 1.9 $\pm$ 0.1 meq/g and a yield of nanofibrillation [27] above 95 %. Dilute suspensions (0.1 wt%) were highly transparent, with a transmittance of 96.1 % at 600 nm.

2.3. Pickering emulsions

Since the effects of nanocellulose concentration and oil concentration on TEO-in-water emulsions were already addressed in a recent work of ours [14], they were kept constant: 10 mL of TEO, 16–60 g of a 1.0 wt % TOCNF suspension, and enough water to make up to 100 g. For TEO/ OFE emulsions, 10 g of water were replaced by the same amount of OFE solution. Likewise, the effect of edible electrolytes was studied by incorporating NaCl (25–600 mM), KCl (100 mM), and sodium citrate (100 mM).

All the emulsions intended for paper coating had the same TOCNF concentration, 0.60 wt%, to ensure their long-term stability. Nonetheless, lower concentration values were studied to determine the minimum value required to emulsify the whole mixture. Likewise, the surface tension of the aqueous phase was estimated from pendant drop assays with a DSA25 device from Krüss Scientific (Hamburg, Germany), on the basis of the Young-Laplace equation [28].

Mixtures were dispersed with an UltraTurrax T25 stirrer (IKA®-Werke GmbH, Staufen, Germany), at an angular speed of 6000 rpm and for 2 min. Then, they were passed once through the HPH at 300 bar and stored at 23 °C for 24 h before any characterization.

2.4. Paper coating

Testliner was cut into 30 cm $\times$ 20 cm rectangular sheets to be coated by means of a K Control Coater (RK Print Coat Instruments, Litlington, United Kingdom). Emulsions were heated to 40 °C to ensure they had no yield stress. Bar coating was performed with a smooth roll (nominal thickness: 20 μm), at 3 m/min and providing excess emulsion (*ca.* 5 mL). At least four sheets were coated for each formulation: TEO emulsion, TEO/OFE emulsion, and three TEO/OFE emulsions with different salt contents (25 mM, 50 mM, and 100 mM).

Uncoated and coated sheets were conditioned at 23 °C and 50 % relative humidity before being tested. Selected samples were visualized by field emission scanning electron microscopy (FE-SEM), by means of a Hitachi S-3000 microscope (Hitachi Europe, Stoke Poges, UK), equipped with a secondary electron detector. The accelerating voltage was set at 7 kV.

2.5. Characterization

2.5.1. Analysis of constituents before emulsifying

The *in vitro* antioxidant activity of both TEO and OFE was tested by the DPPH assay, following the procedure developed in our previous work [14]. All spectrophotometric measurements were carried out with a Shimadzu UV-1280 device.

The total phenolic content (TPC) of TEO and OFE solution was quantified by reduction of the Folin-Ciocalteu reagent in aqueous medium [29]. For that, a known mass of sample was dissolved or dispersed in 8.4 mL of aqueous ethanol (5 vol%), followed by addition of 0.4 mL of Folin-Ciocalteu reagent. Finally, we added 0.6 mL of aqueous sodium carbonate (1 M) and kept the mixture in the dark, at 23 °C and for 120 min. TPC was expressed as mass of gallic acid equivalents (GAE) per gram of sample, comparing the absorbance at 750 nm recorded after each reaction with that attained by gallic acid [30]. The TPC assay was

also executed to roughly assess the OFE/TEO/water liquid-liquid equilibrium at 23 °C with varying ionic strength. For that, emulsions were left undisturbed and in the dark after salt addition for 24 h, and samples were taken from the aqueous phase.

2.5.2. Analysis of emulsions

Nanocellulose-stabilized TEO/OFE emulsions, with and without electrolyte addition, were observed by optical microscopy, involving a Leica DMR-XA microscope (Wetzlar, Germany). Halogen illumination and bright field modes were selected.

The rheological behavior of emulsions was assessed at 23 °C by using two different devices based on concentric cylinders: MCR 302e, from Anton Paar (Graz, Austria), for a very low shear rate range (0.02 s^{-1} to 2 s^{-1}), and RVI-2, from PCE Instruments (Albacete, Spain), for low-to-high shear rate (2.5 s^{-1} to 40 s^{-1}).

Samples of emulsions were left to dry over polystyrene Petri dishes, at 60 °C for 24 h. The resulting films were subjected to Fourier-transform infrared (FTIR) spectroscopy in an Alpha II FTIR device (Bruker, Madrid, Spain), equipped with an ATR module, setting the resolution at 4 cm^{-1}.

2.5.3. Assessment of packaging paper sheets

As it is consuetudinary in coating experiments, all sheets were weighted to calculate the grammage or basis weight, and their thickness was measured by means of a Starrett digital micrometer (Athol, MA, USA). Air permeability of uncoated and coated paper sheets was assessed in accordance with ISO 5636/5 (Gurley method), recording the time needed for 100 cm^3 to pass through 6.45 cm^2 of sample. Roughness was measured by using a Bendtsen tester from Metrotec (Gipuzkoa, Spain) complying to ISO 8791-2. The burst index was quantified with a Mullen tester from IDM (Gipuzkoa, Spain), designed in accordance with ISO 2759 [25]. Opacity was measured by means of a Technibrite Eric 950 colorimeter from Technidyne (New Albany, IN, USA).

2.5.4. Release experiments

Samples of area 0.01 m^2 were cut from coated paper sheets and placed in different aqueous food simulants, as a means to evaluate the intended migration of phenolic compounds. The list of food simulants follows: ethanol 10 vol% (simulant A), acetic acid 3 wt% (simulant B), and ethanol 20 vol% (simulant C). The volume of liquid was 100 cm^3. Extracts were collected at different times during 4 h to assess release kinetics, and then once more after 24 h at 23 °C. Since the influence of removing only 0.5 vol% of the food simulant was neglected, volume was not replenished after sampling.

They were directly used for DPPH inhibition tests, combining 0.5 mL of sample with 3 mL of DPPH 0.2 mM (in ethanol) and 0.5 mL of water. In the case of acetic acid, 0.5 mL of aqueous NaOH (0.5 M) were added instead of water, given that acidic media may cause unreliable results in DPPH inhibition assays [31]. The absorbance at 516 nm was recorded and compared with that of the negative control test, which was performed with food simulant instead of extract. Experiments were performed in triplicate.

2.5.5. Antibacterial activity

Capabilities to inhibit the growth of *E. coli* and *L. monocytogenes* were assessed for TEO, OFE, and nanocellulose-stabilized emulsions, by drop diffusion [32]. Sterilization, inoculation of MH agar with the target culture and diffusion of the potentially antibacterial agent took place as described in a previous work [14]. Briefly, 3 μL of sample were directly placed over a previously inoculated Petri dish. The dish was then protected with Parafilm (Neenah, WI, USA) and incubated at 30 °C for 24 h. The experiment was repeated at least twice for each sample.

For uncoated and coated paper sheets, colorimetric tests of *L. monocytogenes* growth were performed with the *Listeria*-selective chromogenic agar. For that, 50 mm-diameter paper disks were obtained by means of a circular die cutter. Disks were sterilized, inoculated with *L. monocytogenes* (*ca.* 10^7 CFU), and incubated as aforementioned.

Bacterial growth was evidenced by black coloration.

3. Results and discussion

3.1. Bioactive properties of the system's constituents

In absence of TEO and OFE, neither antibacterial activity nor DPPH scavenging activity was observed for TOCNF suspensions. Thus, the role of TOCNFs was that of emulsion stabilizer, rheology modifier, carrier of bioactive compounds, and binder to the packaging paper surface [33]. In turn, testliner sheets did not show antimicrobial properties either. While TPC assays on paper allowed us to reject the null hypothesis, presumably because of remaining lignin, blank extracts did not exert a significant inhibition of DPPH (Table 1).

As already exploited in a previous study [14], TEO has strong antibacterial activity towards both Gram-positive and Gram-negative bacteria. Such activity has been characterized in detail elsewhere [34]. Furthermore, given that its main constituent is a monophenol ring-bearing terpene (thymol), TEO has noteworthy antioxidant properties (Table 1). However, DPPH inhibition with pure TEO was in the same order of magnitude as that attained with the OFE solution (9.1 wt%), which means that the half maximal inhibitory concentration (IC_{50}) of the pure extract was one order of magnitude lower: more precisely, 71 μg/mL. This value is remarkable, since hydroxytyrosol (an excellent antioxidant agent [20]) constituted only 7.0 wt% of OFE and 0.64 wt% of the OFE solution. Nonetheless, although it could be partially explained as a matter of concentration, the OFE solution did not display zones of inhibition against *E. coli* (Fig. S1). In fact, the antimicrobial activity of hydroxytyrosol has been a subject of controversy, with notorious disparity among different studies [35,36].

In short, TEO could be deemed a strong antimicrobial and antioxidant agent, OFE showed excellent antioxidant effects, TOCNFs were found to be neither antioxidant nor antimicrobial, and testliner was mostly a passive support. With the formulation of the emulsions presented here in mind, in which OFE was diluted to 9.1 g/L, it could be stated that TEO accounted for the highest antimicrobial and antioxidant activity *per se*. However, as described in our previous study with TEO [14], its poor water solubility hindered its potential to work as an antioxidant emitter unless the food simulant was ethanol 50 vol% (simulant D1, usually selected for lipophilic foodstuffs [16]). Despite the degree of dilution of olive phenolics in the bifunctional emulsions, their hydrophilic character is what ensures radical scavenging activity without excessive migration for a broad spectrum of potential food products.

3.2. A look at liquid-liquid equilibria

Once TEO, the OFE solution, and water were mixed in the absence of TOCNFs, we observed immediate phase separation due to the low density of TEO (903 g/L). Evidently, there was certain mass transfer of the nonelectrolyte solutes of OFE, including hydroxytyrosol, from the continuous phase to TEO droplets. Likewise, the potential transfer of thymol to the aqueous phase must be assessed. These mass transfer phenomena could be modified by salt addition, affecting the oil/water partition coefficient (or, as preferred by IUPAC, partition ratio) [37].

Results from TPC assays in the aqueous phase revealed differences ranging from a 275-fold to a 520-fold magnitude between TEO/water (6 g–8 g GAE L^{-1}) and TEO/OFE/water systems (2.4 g–2.8 g GAE L^{-1}), as schematized in Fig. 2a. Hence, even though the determination of OFE phenolics was simultaneous with that of TEO phenolics in TEO/OFE/water mixtures, the contribution of the latter to the total was neglected. All results lied above the lower level of quantification [29].

As expected, the partition of thyme phenolics between the oil phase and the water phase favored the former. Nonetheless, while >99.9 % of thyme phenolics remained in TEO, the aqueous phase attained a relatively high concentration of olive phenolics. On a side note, it is clear that each of the individual phenolic components of TEO (such as thymol and carvacrol) and each of the individual phenolic compounds of OFE (such as hydroxytyrosol) has its own behavior, but it is practical to group them as in Fig. 2b. From these plots, two Setschenow-type constants (K_s) can be estimated from a linear fitting to [38]:

$$log\left[\frac{TPC}{TPC_0}\right] = -K_S C_{NaCl} \tag{1}$$

where C_{NaCl} is the molar concentration of salt and TPC_0 is the phenolics concentration in the aqueous phase with no electrolyte addition. For thyme oil, salting-out effects decreased the solubility of phenolic compounds in the aqueous phase, attaining a positive constant: $K_S = 0.20 \pm 0.03$ M^{-1} (adjusted R^2: 0.75). For the more polar olive extracts, those effects were notably lower: $K_S = 0.070 \pm 0.009$ M^{-1} (adjusted R^2: 0.77). In any case, salt addition is a way to concentrate the oil phase, *i.e.*, the dispersed phase once the emulsions were formed, in bioactive compounds. Although this may have some usefulness for controlled release, salting-out effects have been found to be rather mild in comparison to the severe impacts that electrolytes impart on emulsified systems.

The amphiphilic character of OFE is postulated to have aided TOCNFs in the stabilization of TEO/OFE/TOCNF emulsions. As shown in Fig. 3a, the surface tension of the aqueous phase was consistently lower in the presence of amphiphilic extracts. This explains why, when TOCNF concentration was 0.32 wt%, the whole volume of the TEO/OFE/TOCNF emulsion was stabilized, but a millimetric layer of TEO stayed on the top of the TEO/TOCNF emulsion (Fig. 3b, c) [14]. For the latter system (without OFE) to attain macroscopical homogeneity along, the required concentration of nanofibers was 0.40 wt%. The rheological behavior at consistencies higher than 0.40 wt% (high viscosity, occurrence of yield stress) hindered the measurement of the surface tension.

### 3.3. Features of TEO/OFE emulsions with different electrolyte content

A common characteristic of TEO, TEO/OFE, and TEO/OFE/salt mixtures after dispersion with TOCNFs (0.6 wt%), followed by HPH, was the absence of a free oil phase. Likewise, except for the case of sodium citrate, gravity-driven phase separation was avoided for at least eight months. Nanocellulose-stabilized TEO-in-water and TEO/OFE-in-water emulsions were macroscopically homogeneous, and so they were with a moderate ionic strength (NaCl 25 mM, NaCl 50 mM). However, electrolytes imparted creaming effects that were macroscopically detectable at a 100 mM salt concentration. In those cases, TEO/TOCNFs formed agglomerates because of the damping of electrostatic repulsion between nanofibers [39]. Those systems were then not proper emulsions, but "pseudo-emulsions". Still, agglomerates did not settle or float. Instead, they remained suspended in the aqueous serum phase.

As can be seen from Fig. 4, nanocellulose-stabilized emulsions displayed consistently spherical droplets. Nonetheless, they were polydisperse in terms of diameter, encompassing some as large as 40 μm

Table 1
Bioactive characteristics of TEO, OFE solution, and the paper substrate: TPC, IC_{50} for DPPH inhibition, and diameter of the zone of bacterial growth inhibition.

	TPC (mg GAE/g)	IC_{50} (mg/mL)	*L. monocytogenes* inhibition diameter (mm)	*E. coli* inhibition diameter (mm)
TEO	216 ± 9	0.45	27	42
OFE solution	39 ± 1	0.77	12	0
Liner	8 ± 1	Not possible	0	0
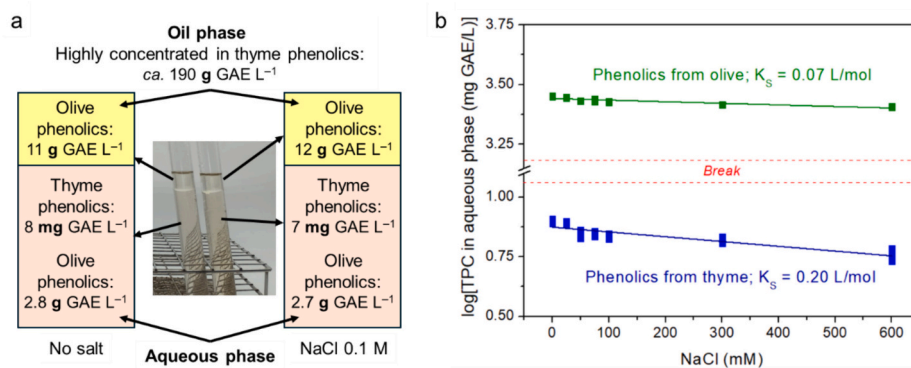
Fig. 2. Study of the concentration of phenolics in each phase: scheme of the partition with and without electrolyte (a); Setschenow-type plots for TPC from TEO and OFE in the aqueous phase.
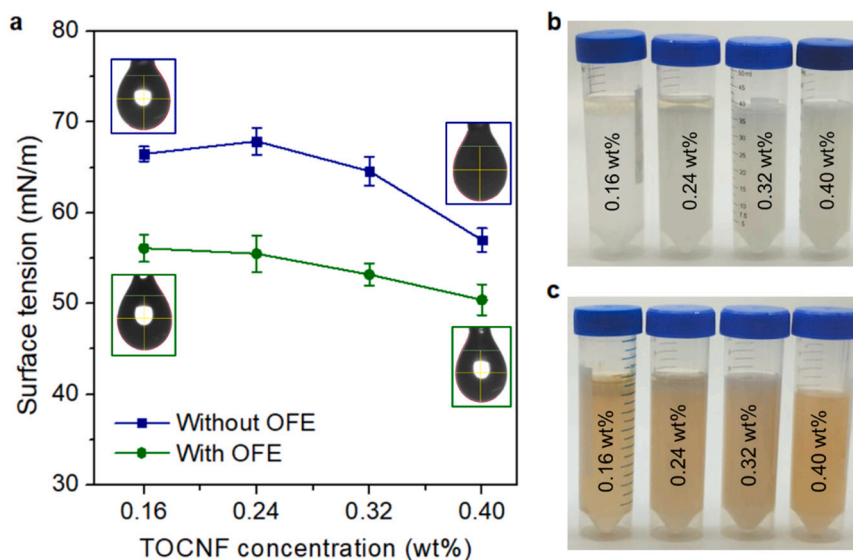
Fig. 3. Surface tension of aqueous CNF suspensions (a), emulsions with TEO of OFE-free suspensions (b), and TEO/OFE/TOCNF systems.

(Fig. 4a) and some below 2 μm (Fig. 4b). The addition of NaCl (25 mM) or KCl (25 mM) caused an overall decrease in particle size (Fig. 4c, d, e), but the same molar concentration of sodium citrate increased the polydispersity (Fig. 4f). In the latter case, the molar ionic strength was 6 times higher (0.15 M), compromising the stability of the emulsion.

The reduction of droplet size with electrolyte addition was observed in a more detailed way by Heise et al. with cellulose nanocrystals [40]. Nonetheless, unlike nanocrystals, nanofibers have a great tendency to entanglement, and thus there was also progressive clustering of the dispersed phase, starting at 50 mM (Fig. 4g) and becoming evident at 100 mM (Fig. 4h). In this sense, the effects of KCl (significantly more conductive) were not qualitatively different from those of NaCl, except for certain loss of sphericity that is appreciated in Fig. S2 (additional micrographs) for the larger drops [39]. Fig. S2 also indicates that when the salt with a 100 mM concentration was sodium citrate, the ionic strength was so high that the generation of massive drop multiplets was visible to the naked eye. Such emulsion could not be deemed stable.

The occurrence of non-coalescing doublets and multiplets (Fig. 4b, d) deserves a mention. According to the DLVO theory, droplets in close contact would coalesce if repulsive electrostatic interactions did not overcome attractive forces [41]. In Pickering emulsions stabilized by TOCNFs, this electrostatic repulsion is provided by the negatively-charged carboxylate groups. This is why non-coalescing doublets were hardly found in systems where the ionic strength was 50 mM or higher (Fig. 4e–h).

The ATR-FTIR of the paper substrate and the oven-dried emulsions are displayed in Fig. 5. A thoughtful analysis of each band is out of the scope, but the most relevant ones are highlighted. The broad band at 3328 cm^{-1} is associated with hydrogen-bonded O—H stretching [42]. It was more intense for nanocellulose than for testliner's cellulose. Likewise, absorption near 1423 cm^{-1} is related to crystalline cellulose I [43]. In all cases, the most prominent peak was the one due to C—O—C vibrations in the cellulose backbone (1026 cm^{-1}). The band at 1610 cm^{-1} for TOCNFs and films from Pickering emulsions owes to C=O stretching in carboxylate groups [44].

Samples with TEO or TEO/OFE, additionally, displayed an absorption band at 812 cm^{-1}, related to bonds between phenyl rings and their substituents, and several bands around 2966 cm^{-1}, attributed to C—H stretching. Nonetheless, most of the characteristic absorption bands of phenolic compounds, including O—H stretching (*ca.* 3330 cm^{-1}), were overlapped by those of cellulose. More interestingly, the band at 1734 cm^{-1} is not found for pure thymol, but it results from a hypsochromic shift arising from cellulose-thymol interactions [45]. Salt addition, even to a great extent (100 mM), resulted in a qualitatively similar spectrum. It is observed, however, that the absorption bands assigned to aromatic moieties became more intense. In other words, electrolytes increased the proportion of phenolics attained at equilibrium moisture.
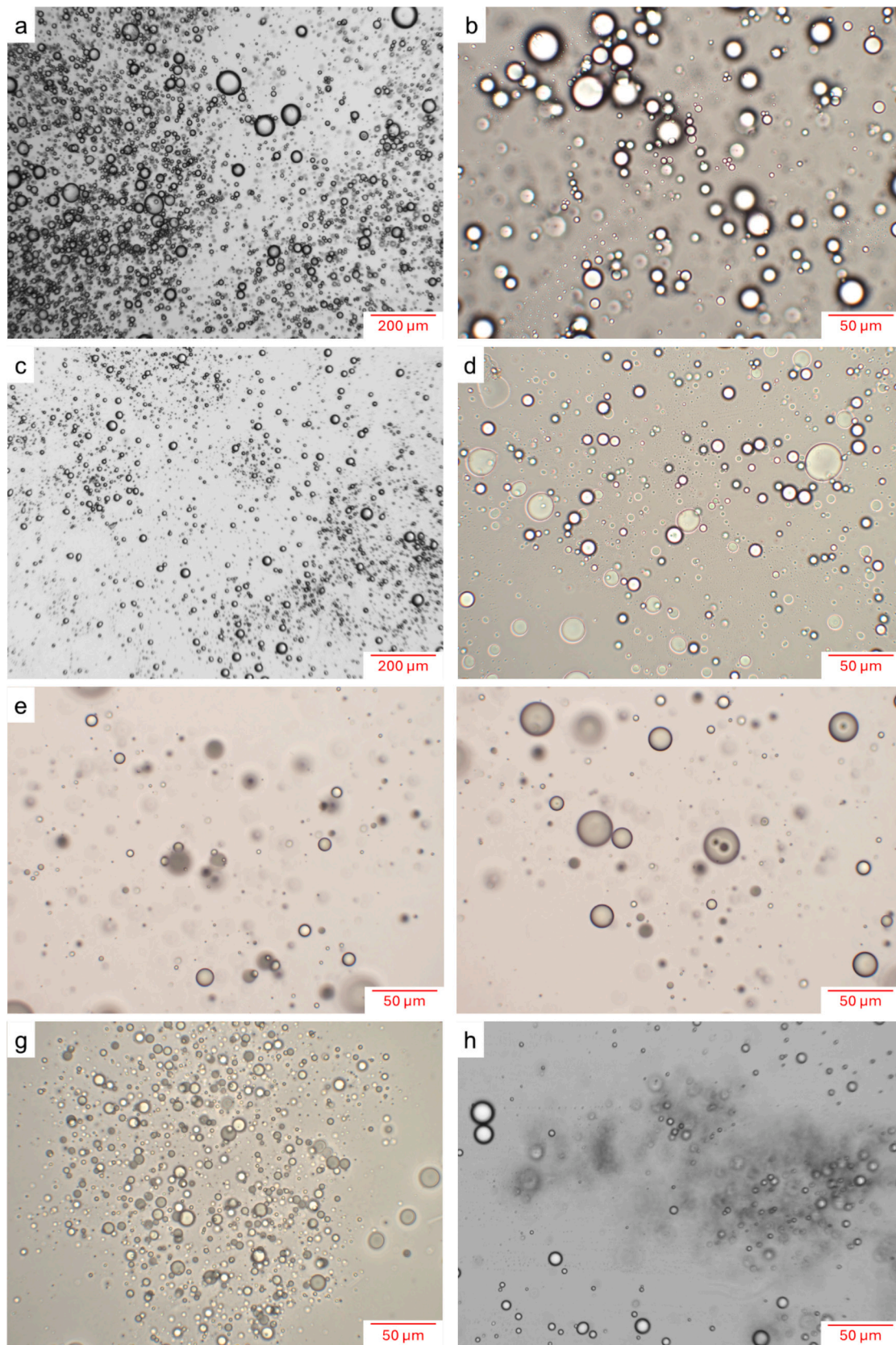
Fig. 4. Optical micrographs of TEO/OFE/TOCNFs water emulsions (a,b), and effect of the addition of NaCl 25 mM (c,d), KCl 25 mM (e), and sodium citrate 25 mM (f), NaCl 50 mM (g), NaCl 100 mM (h).
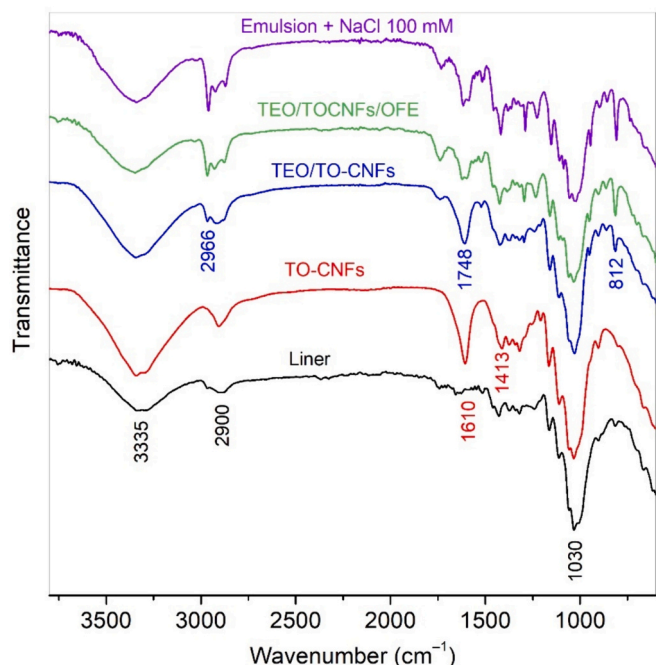
Fig. 5. Normalized and vertically shifted ATR-FTIR spectra of the packaging paper, nanocellulose films, nanocellulose-stabilized TEO films, and nanocellulose-stabilized films with TEO in the dispersed phase and OFE in the continuous phase.

3.4. Rheological behavior

Taking into account the rheology of emulsions is of the essence for their own stability and to be applied in paper coating. On one hand, viscous forces (Stokes' drag) oppose the excess gravitational force of the continuous phase against the dispersed phase, to the point that having a significant yield stress can prevent phase separation indefinitely. On the other, the coat weight attained by bar coating is known to increase with the apparent viscosity of the coating emulsion/suspension, but excessive thickening hampers applicability [46].

Nanocellulose-stabilized TEO/OFE emulsions had shear-thinning behavior, regardless of the presence of electrolytes, and thixotropic character. The decrease in apparent viscosity with time, while subjected to shear stress (τ), is shown in Fig. 6 for two levels of shear rate (γ). The

time at which the system approached an equilibrium viscosity depended on the shear rate: *ca.* 94 s for $\dot{\gamma} = 2.5\ \mathrm{s}^{-1}$ and *ca.* 16 s for $\dot{\gamma} = 45\ \mathrm{s}^{-1}$. In the latter case, the presence of electrolytes seemed to quicken it. What was obvious from the addition of NaCl or KCl was the decrease in apparent viscosity, in a non-linear fashion with salt concentration. Furthermore, for a 100 mM concentration, KCl reduced the viscosity to a slightly higher extent than NaCl, likely due to the higher mobility of the potassium ion ($7.6 \cdot 10^{-8}\ \mathrm{m^2\ s^{-1}\ V^{-1}}$) in comparison with the sodium ion ($5.2 \cdot 10^{-8}\ \mathrm{m^2\ s^{-1}\ V^{-1}}$) [47].

Besides shear-thinning and certain time-dependent behavior, emulsions displayed yield stress (τ_0), at least in the absence of electrolytes. Their apparent viscosity (η) could be fitted to an adaptation of the Ostwald-De Waele power law:

$$\tau = \tau_0 + K\dot{\gamma}^n \tag{2}$$

where K is the consistency index and n is the flow behavior index. Generally, it is more practical, and even more accurate, to infer τ_0 from the intersection with the vertical axis in shear stress-shear rate plots below 2 s^{-1} (Fig. S3), and then input it as a fixed parameter in the fitting software (in this case, OriginLab's OriginPro 8.5). For salt concentrations equal or >50 mM, no yield stress was appreciated (Table 2). Furthermore, besides the expected decrease in the consistency index, the addition of NaCl diminished the flow behavior index from 0.34 to 0.11–0.15. In other words, electrolytes accentuated the shear-thinning behavior of nanocellulose-stabilized emulsions.

The most plausible mechanism by which a higher ionic strength decreased the apparent viscosity and the yield stress of emulsions is the diminishment of electroviscous effects [33,48]. Because of electric-field screening, long-range interactions between the carboxylate groups of TOCNFs and surrounding water molecules were severely weakened. Hence, TOCNFs caught much less water than what they did in low conductivity media. However, instead of observing oil/water phase separation with the disappearance of the yield stress, TEO/OFE/TOCNFs

Table 2
Rheological properties of nanocellulose-stabilized suspensions.

Emulsion	NaCl (mM)	τ_0 (Pa)	K (Pa·s^{-n})	n
TEO/TOCNFs in water	0	1.3	12.8 ± 3	0.32 ± 0.02
TEO/OFE/TOCNFs in water	0	0.7	8.1 ± 0.5	0.34 ± 0.05
	25	0.2	6.6 ± 0.5	0.14 ± 0.06
	50	0	4.36 ± 0.02	0.15 ± 0.01
	100	0	3.37 ± 0.07	0.11 ± 0.02
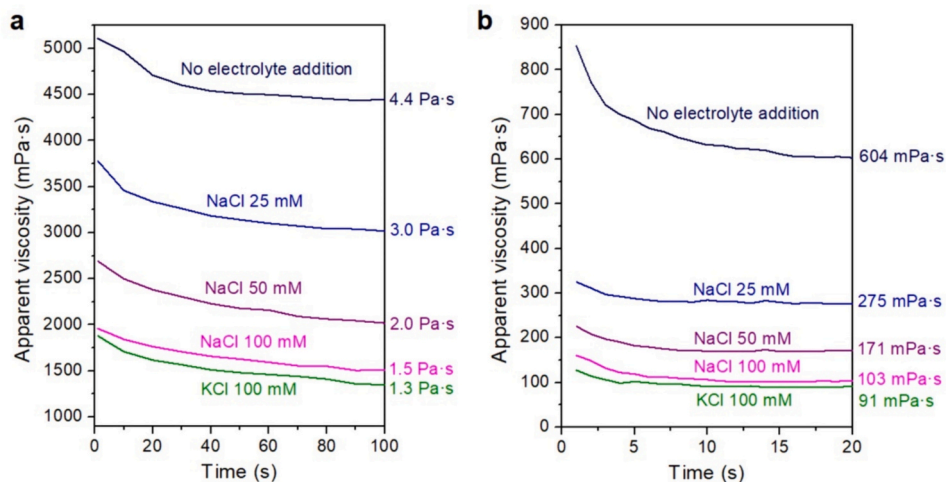
Fig. 6. Thixotropy of nanocellulose-stabilized emulsions at a shear rate of 2.5 s^{-1} (a) and at a shear rate of 45 s^{-1} (b), evidencing the effect of salt addition and the shear-thinning behavior.

kept occupying the whole volume of the emulsion at least eight months after preparation, with or without NaCl. It can be followed that, as TOCNF/water interactions became weaker, TOCNF/oil interfacial adsorption became more entropically and enthalpically favored [23].

3.5. Passive packaging properties of coated paper

Although the main purpose of nanocellulose-stabilized TEO/OFE emulsions was attaining paper-based active packaging, its barrier properties and its mechanical properties are always important to ensure proper protection of foodstuffs [49,50]. Although it owed more to nanofibers than to the oil and the extract, paper coating with either TEO/TOCNFs or TEO/OFE/TOCNFs smoothened the surface, improved air barrier properties, and even provided a slight enhancement of burst resistance (Table 3).

Despite their low viscosity, electrolyte-containing emulsions attained nearly the same coat weight as salt-free systems (5–7 g m^{-2}), as shown in Table 3. This was due to the crystallization of salt over the paper surface, which compensated the lower amount of TEO and OFE. Crystals roughened the surface of paper packaging and TEO/TOCNF aggregates produced an uneven coating thickness, as shown by the high standard deviations. What is worse, the agglomeration of nanofibers produced by electric-field screening resulted in unhindered pathways for air permeability. Hence, barrier properties to air decreased from 105 to 108 Gurley s down to 49 s per 100 cm^3 of air. Furthermore, considering the hygroscopic nature of sodium chloride, an external hydrophobic layer would be necessary to protect foodstuffs from moisture [51].

The reduction of porosity attained by the TEO/OFE/TOCNF coating, without salts, is evident in the micrographs of Fig. 7. The space between fibers in Fig. 7a (uncoated) was closed down and TOCNF aggregates, formed during the drying process, are evident in Fig. 7b, c. Fig. 7d highlights the coating layer over base paper.

Even though electrolyte addition was overall detrimental to barrier properties, it is still worthy of consideration because of the lower droplet size, the possibility to adjust the rheological behavior and, as developed in the following section, the potentiation of antimicrobial activity. In fact, NaCl has been used in polypropylene-based packaging with good results in terms of shelf-life extension [52].

Finally, another passive property that could be easily overlooked, but with great importance for the preservation of OFE, is opacity. Hydroxytyrosol is photodegraded if exposed to sunlight or other sources of ultraviolet radiation [53]. In this sense, the choice of high-grammage packaging paper assured that the opacity was 94 ± 1 %, regardless of coating compositions.

3.6. Antibacterial activity of coated paper

As aforementioned, neither paper nor TOCNFs showed appreciable inhibition of L. *monocytogenes* after inoculation and incubation. However, paper sheets coated with nanocellulose-stabilized TEO-in water emulsions inhibited the growth of this Gram-positive bacteria to a great extent, an extent that was further increased with OFE and NaCl. This is displayed in Fig. 8, along with the CFU count (in tens of thousands) in each case [54].

The antimicrobial activity of thymol has been previously reported [55], while that of the OFE solution was individually assessed for L. *monocytogenes* in this study (Table 1). The antibacterial properties of NaCl or KCl (Fig. S1), including those specific to this microorganism, have long been well-known [56]. However, while their presence in food packaging is allowed and the EU has not set specific migration limits for them [57], they are evidently subjected to the overall restrictions and possess the risk of sensory impacts [58]. Unlike in the case of antimicrobial NaCl-containing polypropylene films [52], the migration of ions to hydrophilic food products was not hindered by TOCNF-based coatings, potentially affecting their salinity and their taste.

In any case, salt addition was not necessary to significantly extend the shelf life of foodstuffs, considering that the TEO/OFE/TOCNF-coatings of without electrolytes (Fig. 8c) already attained a reduction in CFU by two orders of magnitude with respect to the blank (Fig. 8a). Such inhibition of L. *monocytogenes* is of utmost importance for consumer protection, as it contributes to the prevention of listeriosis, sepsis, meningitis, encephalitis, spontaneous abortion, and gastroenteritis [59,60].

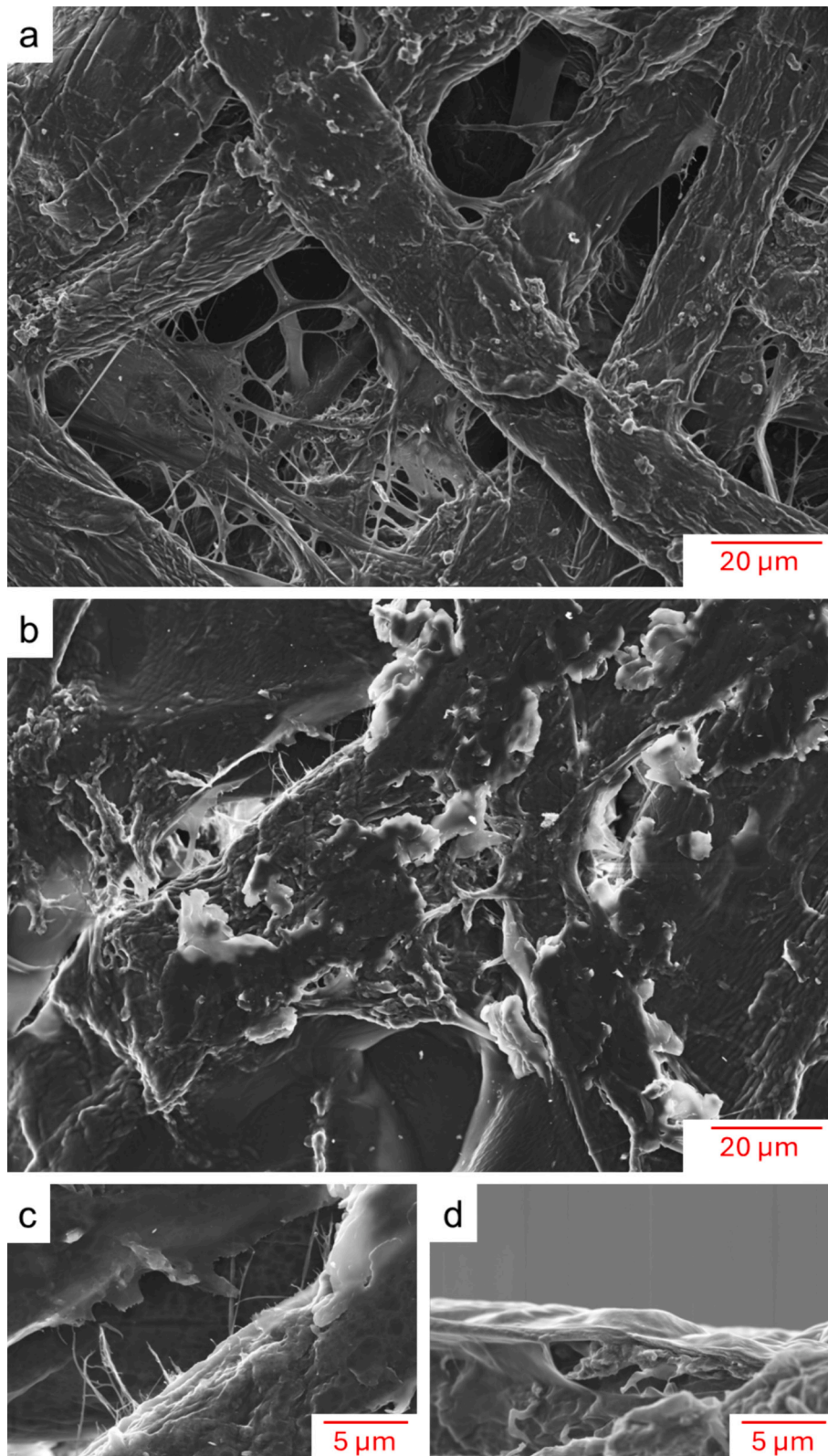### 3.7. Radical scavenging activity of coated paper

Regarding *in vitro* antioxidant properties, both TEO and the OFE solution showed remarkable inhibition of the DPPH radical. The limitation of TEO/CNF-coated paper lies in the poor release of this lipophilic essential oil to hydrophilic media, which is why DPPH assays were limited to food simulant D1 (ethanol 50 vol%) in our previous publication [14]. In contrast, the amphiphilicity of OFE, as shown above (Fig. 2), favored its intended migration to aqueous phase. Consistently, following 24 h of exposure, Fig. 9a displays inhibition levels between 20 ± 3 % and 27 ± 2 % for foods simulants A (ethanol 10 vol%), B (acetic acid 3 wt%), and C (ethanol 20 vol%). Fig. 9b compares the values attained after 24 h with those of emulsion films of the same area (0.01 m^2), which corresponded to 0.26 ± 0.03 g. Spectra for negative control tests are shown in Fig. S4.

Half-maximum inhibition was not attained in typical paper packaging-to-simulant proportions (0.01 m^2 in 100 mL), but the values reached are high enough to expect significant protection of lipids and other biological macromolecules prone to oxidative stress [61]. In fact, in order to inhibit the DPPH radical beyond 50 %, the necessary area of TEO/TOCNF-coated paper (without OFE) in contact with 100 mL of food simulant D1 was *ca.* 0.025–0.030 m^2 [14].

Not less importantly, the antioxidant constituents of TEO, mainly thymol and carvacrol [62], are more volatile than their counterparts in OFE, mainly hydroxytyrosol [19]. Hence, while a significant part of the TEO placed by coating evaporates along with water during drying, the long-term permanence of OFE is granted by its much lower vapor pressure. In addition, the concentration of OFE required to attain 20–27 % DPPH inhibition is lower than the overall migration limit (10 mg/dm^2), and also than the average recognition threshold of olive polyphenols (8 mg/100 g), which provide bitter taste if their concentration is high enough [63].

Attending to the rate of enrichment of the liquid phase in antioxidant compounds, there was burst release in all cases, since the first sample (after 6 min) already reached roughly one third of the maximum

Table 3
Passive packaging properties of uncoated testliner sheets, sheets coated with TEO-in-water emulsions, and sheets coated with the bifunctional emulsions presented in this study. Tolerance intervals correspond to twice the standard deviation.

| Coating	NaCl (mM)	Basis weight (g m^{-2})	Thickness (μm)	Burst index (kPa m^2 g^{-1})	Roughness (mL/min)	Air resistance (s/100 cm^3)
None	0	170 ± 1	249 ± 3	2.0	760 ± 40	33.4 ± 0.6
TEO/TOCNFs	0	176 ± 1	260 ± 4	2.3	500	105 ± 5
TEO/OFE/TOCNFs	0	177 ± 1	259 ± 3	2.2	450	108 ± 4
	25	175 ± 2	264 ± 4	2.1	680 ± 70	75 ± 5
	50	176 ± 2	264 ± 8	2.2	710 ± 70	60 ± 3
	100	175 ± 3	261 ± 9	2.1	800 ± 80	49 ± 2

Fig. 7. FE-SEM images of the surface of uncoated paper (a), the surface of TEO/OFE/TOCNF-coated paper (b), interfiber space in coated paper (c), and cryo-section of coated paper (d).

inhibition attained. Although several kinetic models would provide a satisfactory fit, the straight lines in Fig. 9 ($R^2 > 0.95$) correspond to power law equations of the form [64]:

$$\frac{\text{Inhibition (t)}}{\text{Inhibition (24 h)}} = k\, t^n \forall 0 \leq t \leq 4\ h \tag{3}$$

The empirical coefficient k was 0.55, 0.67 and 0.52 h^{-n} for food
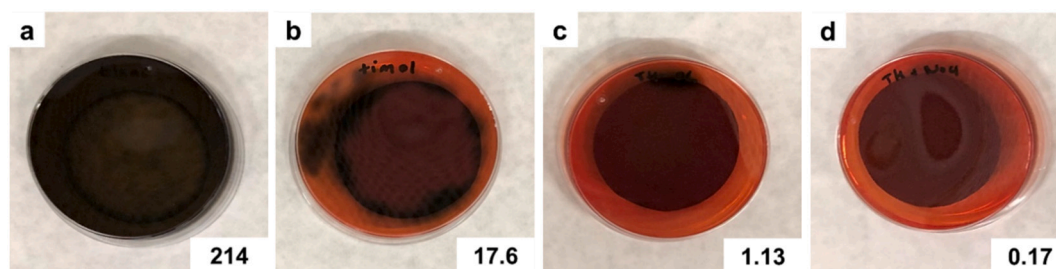
Fig. 8. Growth inhibition of *L. monocytogenes* on chromogenic agar medium with the blank paper (a), TEO/TOCNF-coated paper (b), TEO/OFE/TOCNF-coated paper (c), and paper coated with the emulsion plus NaCl 50 mM (d). Inset numbers account for 10^4 CFU (average of three measurements).
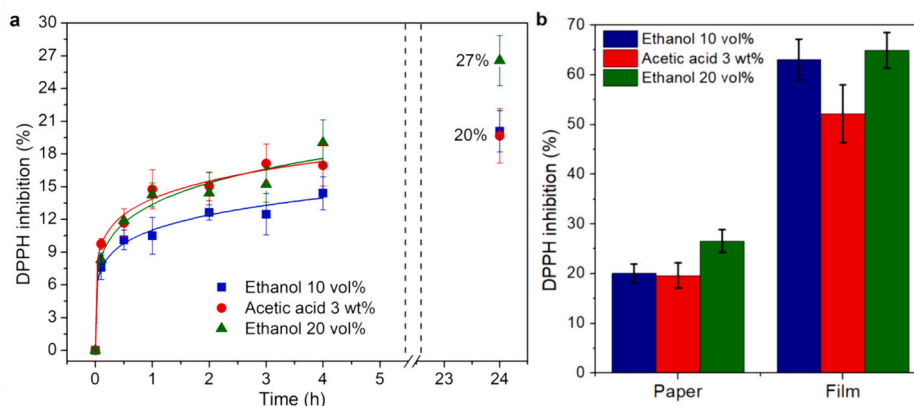
Fig. 9. Radical scavenging assays (on DPPH 0.167 mM) with hydrophilic food simulants in contact with TEO/OFE/TOCNF-coated paper, after different sampling times (a), and comparison after 24 h with an emulsion film of the same composition and area (b).

simulants A, B and C, respectively. The corresponding values for the empirical exponent *n* were 0.17, 0.20 and 0.16. It can be concluded that the release of antioxidant compounds to simulant B was faster than their release to simulants A and C. Nonetheless, migration to aqueous-alcoholic systems significantly continued overnight, while the release to acetic acid 3 wt% approached its maximum value after only 3 h. There is overlapping, to an extent higher than 40 %, between the tolerance interval of this value and the tolerance interval of the value at 24 h.

4. Conclusions

Two sources of bioactive compounds were synergistically combined in TOCNF-stabilized emulsions. On one hand, the emulsified oil was TEO: immiscible with water, lipophilic, possessing fair antioxidant activity (IC$_{50}$ = 0.45 mg/L), and as previously known, capable of inhibiting the growth of a broad spectrum of Gram-negative and Gram-positive bacteria. On the other hand, OFE was initially dissolved in the aqueous phase, but, due to its amphiphilic character, it was similarly distributed between the two phases at equilibrium. By decreasing the surface tension of the aqueous phase, this amphiphilicity lowered the minimum concentration of TOCNFs required to observe macroscopic homogeneity over the whole volume of the emulsion. Furthermore, OFE enhanced the inhibition of *L. monocytogene* and provided a stronger antioxidant activity per unit of mass migrated to the food simulant.

In the absence of strong electrolytes, stable emulsions were highly viscous, thixotropic, with shear-thinning behavior, and with yield stress. The latter could be related to the resistance of emulsions to phase separation. Then, the addition of edible salts not only decreased the apparent viscosity (from 4.4 to 3.0 Pa·s in the case of low shear rate and NaCl 50 mM), but also suppressed the yield strength and reduced the concentration of phenolics in the aqueous phase. Still, Pickering emulsions remained stable and even with lower droplet size. Hence, it is inferred that electric-field screening improved adsorption of TOCFNs at

the oil/water interface. However, the diminishment of electrostatic repulsion favored the heterogeneous clustering of non-coalescing droplets.

Packaging paper coated with these bifunctional emulsions successfully inhibited the growth of *L. monocytogenes*, a common foodborne pathogen, and released radical scavengers to food simulants A, B, and C. This was a key consequence of incorporating OFE, since TEO/TOCNF-coated paper had been proved to require lipophilic simulants (such as D1) to attain high levels of antioxidant activity. Release was more sustained to aqueous-alcoholic media (A, B) than to aqueous acetic acid (C), for which the value recorded after 3 h was not significantly different from that after 24 h.

CRediT authorship contribution statement

Roberto J. Aguado: Writing – original draft, Software, Methodology, Investigation, Formal analysis, Data curation, Conceptualization. **Elena Saguer:** Writing – review & editing, Visualization, Validation, Methodology, Investigation. **Quim Tarrés:** Writing – review & editing, Visualization, Investigation, Data curation. **Núria Fiol:** Writing – review & editing, Validation, Software, Resources, Formal analysis. **Marc Delgado-Aguilar:** Writing – review & editing, Visualization, Validation, Supervision, Resources, Project administration, Methodology, Funding acquisition.

Declaration of competing interest

The authors declare that they have no known competing financial interests or personal relationships that could have appeared to influence the work reported in this paper.

Data availability

All data displayed in the article, as supplementary information, or else available upon request.

Acknowledgements

Appendix A. Supplementary data

Supplementary data to this article can be found online at https://doi.org/10.1016/j.ijbiomac.2024.135110.

References

[1] S. Casalini, M.G. Baschetti, M. Cappelletti, A.C. Guerreiro, C.M. Gago, S. Nici, M. D. Antunes, Antimicrobial activity of different nanocellulose films embedded with thyme, cinnamon, and oregano essential oils for active packaging application on raspberries, Front Sustain Food Syst 7 (2023), https://doi.org/10.3389/fsufs.2023.1190979.

[2] L. Atarés, A. Chiralt, Essential oils as additives in biodegradable films and coatings for active food packaging, Trends Food Sci Technol 48 (2016) 51–62, https://doi.org/10.1016/j.tifs.2015.12.001.

[3] M.A. Herrera, A.P. Mathew, K. Oksman, Barrier and mechanical properties of plasticized and cross-linked nanocellulose coatings for paper packaging applications, Cellulose 24 (2017) 3969–3980, https://doi.org/10.1007/s10570-017-1405-8.

[4] Q. Tarrés, N. Pellicer, A. Balea, N. Merayo, C. Negro, A. Blanco, M. Delgado-Aguilar, P. Mutjé, Lignocellulosic micro/nanofibers from wood sawdust applied to recycled fibers for the production of paper bags, Int. J. Biol. Macromol. 105 (2017) 664–670, https://doi.org/10.1016/j.ijbiomac.2017.07.092.

[5] EUR-LEX, Directive (EU) 2015/720 of the European Parliament and of the Council of 29 April 2015 amending Directive 94/62/EC as regards reducing the consumption of lightweight plastic carrier bags, Official Journal of the European Union (2015). https://eur-lex.europa.eu/eli/dir/2015/720/oj (accessed June 6, 2024).

[6] EUR-LEX, Directive (EU) 2019/904 of the European Parliament and of the Council of 5 June 2019 on the reduction of the impact of certain plastic products on the environment, Official Journal of the European Union (2019). https://eur-lex.europa.eu/eli/dir/2019/904/oj (accessed June 6, 2024).

[7] EUR-LEX, Regulation (EU) 2020/852 of the European Parliament and of the Council of 18 June 2020 on the establishment of a framework to facilitate sustainable investment, and amending Regulation (EU) 2019/2088, Official Journal of the European Union (2020). http://data.europa.eu/eli/reg/2020/852/oj (accessed June 6, 2024).

[8] J. Liu, Y. Yang, L. An, Q. Liu, J. Ding, The value of China's legislation on plastic pollution prevention in 2020, Bull. Environ. Contam. Toxicol. 108 (2022) 601–608, https://doi.org/10.1007/s00128-021-03366-6.

[9] M. Aouay, R.J. Aguado, G. Bayés, N. Fiol, J.-L. Putaux, S. Boufi, M. Delgado-Aguilar, In-situ synthesis and binding of silver nanoparticles to dialdehyde and carboxylated cellulose nanofibrils, and active packaging therewith, Cellulose 31 (2024), https://doi.org/10.1007/s10570-024-05918-5.

[10] J. Jung, G.M. Raghavendra, D. Kim, J. Seo, One-step synthesis of starch-silver nanoparticle solution and its application to antibacterial paper coating, Int. J. Biol. Macromol. 107 (2018) 2285–2290.

[11] F. Aguilar, R. Crebelli, A. Di Domenico, M.W. and M.Y. Birgit Dusemund, Maria Jose Frutos, Pierre Galtier, David Gott, Ursula Gundert-Remy, Claude Lambré, Jean-Charles Leblanc, Oliver Lindtner, Peter Moldeus, Alicja Mortensen, Pasquale Mosesso, Agneta Oskarsson, Dominique Parent-Massin, Ivan Stankovic, Ine Wa, Scientific opinion on the re-evaluation of silver (E 174) as food additive, EFSA J. 14 (2016) 4364, https://doi.org/10.2903/j.efsa.2016.4364.

[12] I. Kostova, V. Lasheva, D. Georgieva, S. Damyanova, A. Stoyanova, S. Stefanov, O. Gulbenia, Antimicrobial active packaging based on dill weed essential oil, Cellul. Chem. Technol. 54 (2020) 347–354, https://doi.org/10.35812/CelluloseChemTechnol.2020.54.35.

[13] G. da S. Ferreira, D.J. da Silva, A.G. Souza, E.D.C. Yudice, I.B. de Campos, R.D. Col, A. Mourão, H.S. Martinho, D.S. Rosa, Eco-friendly and effective antimicrobial Melaleuca alternifolia essential oil Pickering emulsions stabilized with cellulose nanofibrils against bacteria and SARS-CoV-2, Int. J. Biol. Macromol. 243 (2023) 125228, https://doi.org/10.1016/j.ijbiomac.2023.125228.

[14] R.J. Aguado, E. Saguer, N. Fiol, Q. Tarrés, M. Delgado-Aguilar, Pickering emulsions of thyme oil in water using oxidized cellulose nanofibers: towards bio-based active packaging, Int. J. Biol. Macromol. 263 (2024) 130319, https://doi.org/10.1016/j.ijbiomac.2024.130319.

[15] Federal Register, Thymol, Exemption From the Requirement of a Tolerance, https://www.federalregister.gov/documents/2022/09/07/2022-19294/thymol-exemption-from-the-requirement-of-a-tolerance, 2022. (Accessed 27 July 2023).

[16] X.-L. Huang, Z.-W. Wang, C.-Y. Hu, Y. Zhu, J. Wang, Factors affecting migration of contaminants from paper through polymer coating into food simulants, Packag. Technol. Sci. 26 (2013) 23–31, https://doi.org/10.1002/pts.1993.

[17] T. Taguri, T. Tanaka, I. Kouno, Antibacterial Spectrum of plant polyphenols and extracts depending upon Hydroxyphenyl structure, Biol. Pharm. Bull. 29 (2006) 2226–2235, https://doi.org/10.1248/bpb.29.2226.

[18] S. De-Montijo-Prieto, A.M. Gómez-Caravaca, E.J. Guerra-Hernandez, M. Jiménez-Valera, B. Garcia-Villanova, A. Ruiz-Bravo, V. Verardo, Essential oils from fruit and vegetables, aromatic herbs, and spices: composition, antioxidant, and antimicrobial activities, Biology (Basel) 10 (2021) 1091, https://doi.org/10.3390/biology10111091.

[19] M. Rada, Á. Guinda, J. Cayuela, Solid/liquid extraction and isolation by molecular distillation of hydroxytyrosol from Olea europaea L. leaves, Eur. J. Lipid Sci. Technol. 109 (2007) 1071–1076, https://doi.org/10.1002/ejlt.200700061.

[20] S.J. Rietjens, A. Bast, J. De Vente, G.R.M.M. Haenen, The olive oil antioxidant hydroxytyrosol efficiently protects against the oxidative stress-induced impairment of the NO• response of isolated rat aorta, Am. J. Physiol. Heart Circ. Physiol. (2007), https://doi.org/10.1152/ajpheart.00755.2006.

[21] A.G. de Souza, R.R. Ferreira, E.S.F. Aguilar, L. Zanata, D. dos S. Rosa, Cinnamon Essential Oil Nanocellulose-Based Pickering Emulsions: Processing Parameters Effect on Their Formation, Stabilization, and Antimicrobial Activity, Polysaccharides 2 (2021) 608–625. doi:https://doi.org/10.3390/polysaccharides2030037.

[22] H. Yu, G. Huang, Y. Ma, Y. Liu, X. Huang, Q. Zheng, P. Yue, M. Yang, Cellulose nanocrystals based clove oil Pickering emulsion for enhanced antibacterial activity, Int. J. Biol. Macromol. 170 (2021) 24–32, https://doi.org/10.1016/j.ijbiomac.2020.12.027.

[23] I. Capron, O.J. Rojas, R. Bordes, Behavior of nanocelluloses at interfaces, Curr Opin colloid, Interface Sci. 29 (2017) 83–95, https://doi.org/10.1016/j.cocis.2017.04.001.

[24] I. Kalashnikova, H. Bizot, P. Bertoncini, B. Cathala, I. Capron, Cellulosic nanorods of various aspect ratios for oil in water Pickering emulsions, Soft Matter 9 (2013) 952–959, https://doi.org/10.1039/C2SM26472B.

[25] ISO, ISO TC/6: Paper, Board and Pulps, International Standardization Organization, Geneva (Switzerland), 2011.

[26] A. Mazega, A.F. Santos, R. Aguado, Q. Tarrés, N. Fiol, M.À. Pèlach, M. Delgado-Aguilar, Kinetic study and real-time monitoring strategy for TEMPO-mediated oxidation of bleached eucalyptus fibers, Cellulose 30 (2023) 1421–1436, https://doi.org/10.1007/s10570-022-05013-7.

[27] G. Signori-Iamin, A.F. Santos, M.L. Corazza, R. Aguado, Q. Tarrés, M. Delgado-Aguilar, Prediction of cellulose micro/nanofiber aspect ratio and yield of nanofibrillation using machine learning techniques, Cellulose (2022), https://doi.org/10.1007/s10570-022-04847-5.

[28] J.D. Berry, M.J. Neeson, R.R. Dagastine, D.Y.C. Chan, R.F. Tabor, Measurement of surface and interfacial tension using pendant drop tensiometry, J. Colloid Interface Sci. 454 (2015) 226–237, https://doi.org/10.1016/j.jcis.2015.05.012.

[29] M. Pérez, I. Dominguez-López, R.M. Lamuela-Raventós, The Chemistry Behind the Folin–Ciocalteu Method for the Estimation of (Poly)phenol Content in Food: Total Phenolic Intake in a Mediterranean Dietary Pattern, J. Agric. Food Chem. 71 (2023) 17543–17553. doi:https://doi.org/10.1021/acs.jafc.3c04022.

[30] F. AlJuhaimi, I.A. Mohamed Ahmed, M.M. Özcan, E. Uslu, E. Karrar, Effects of maturation on bioactive properties, phenolic compounds, fatty acid compositions and nutrients of unripe and ripe sumac (Rhus coriaria L.) fruits, Food and Humanity 2 (2024) 100281, https://doi.org/10.1016/j.foohum.2024.100281.

[31] K.M. Schaich, X. Tian, J. Xie, Hurdles and pitfalls in measuring antioxidant efficacy: a critical evaluation of ABTS, DPPH, and ORAC assays, J Funct Foods 14 (2015) 111–125, https://doi.org/10.1016/j.jff.2015.01.043.

[32] E. Abdollahzadeh, A. Nematollahi, H. Hosseini, Composition of antimicrobial edible films and methods for assessing their antimicrobial activity: a review, Trends Food Sci. Technol. 110 (2021) 291–303, https://doi.org/10.1016/j.tifs.2021.01.084.

[33] R.J. Aguado, A. Mazega, Q. Tarrés, M. Delgado-Aguilar, The role of electrostatic interactions of anionic and cationic cellulose derivatives for industrial applications: a critical review, Ind. Crop. Prod. 201 (2023) 116898, https://doi.org/10.1016/j.indcrop.2023.116898.

[34] M. Božik, P. Nový, P. Klouček, Chemical composition and antimicrobial activity of cinnamon, thyme, oregano and clove essential oils against plant pathogenic Bacteria, Acta Univ. Agric. Silvic. Mendelianae Brun. 65 (2017) 1129–1134, https://doi.org/10.11118/actaun201765041129.

[35] M.S. Medina-Martínez, P. Truchado, I. Castro-Ibáñez, A. Allende, Antimicrobial activity of hydroxytyrosol: a current controversy, Biosci. Biotechnol. Biochem. 80 (2016) 801–810, https://doi.org/10.1080/09168451.2015.1116924.

[36] N. Zorić, I. Kosalec, The antimicrobial activities of Oleuropein and Hydroxytyrosol BT-promising antimicrobials from natural products, in: M. Rai, I. Kosalec (Eds.), Promising Antimicrobials from Natural Products, Springer International Publishing, Cham, 2022, pp. 75–89, https://doi.org/10.1007/978-3-030-83504-0_5.

[37] A. Berthod, N. Mekaoui, Distribution ratio, distribution constant and partition coefficient, Countercurrent chromatography retention of benzoic acid, J Chromatogr A 1218 (2011) 6024–6030, https://doi.org/10.1016/j.chroma.2010.12.027.

[38] A. Burant, G.V. Lowry, A.K. Karamalidis, Measurement of Setschenow constants for six hydrophobic compounds in simulated brines and use in predictive modeling for

oil and gas systems, Chemosphere 144 (2016) 2247–2256, https://doi.org/10.1016/j.chemosphere.2015.10.115.

[39] D. Takács, M. Adžić, N. Omerović, M. Vraneš, J. Katona, M. Pavlović, Electrolyte-induced aggregation of zein protein nanoparticles in aqueous dispersions, J. Colloid Interface Sci. 656 (2024) 457–465, https://doi.org/10.1016/j.jcis.2023.11.123.

[40] K. Heise, C. Jonkergouw, E. Anaya-Plaza, V. Guccini, T. Pääkkönen, M.B. Linder, E. Kontturi, M.A. Kostiainen, Electrolyte-controlled permeability in Nanocellulose-stabilized emulsions, Adv. Mater. Interfaces 9 (2022) 2200943, https://doi.org/10.1002/admi.202200943.

[41] T. Tadros, Colloid and interface aspects of pharmaceutical science, in: H. Ohshima, K.B.T.-C. and I.S. in P.R. and D. Makino (Eds.), Colloid and Interface Science in Pharmaceutical Research and Development, Elsevier, Amsterdam, 2014: pp. 29–54. doi:https://doi.org/10.1016/B978-0-444-62614-1.00002-8.

[42] J.J. Cael, J.L. Koenig, J. Blackwell, Infrared and raman spectroscopy of carbohydrates, Carbohydr. Res. (1974), https://doi.org/10.1016/s0008-6215(00)82465-9.

[43] A. Kljun, T.A.S. Benians, F. Goubet, F. Meulewaeter, J.P. Knox, R.S. Blackburn, Comparative analysis of crystallinity changes in cellulose I polymers using ATR-FTIR, X-ray diffraction, and carbohydrate-binding module probes, Biomacromolecules 12 (2011) 4121–4126, https://doi.org/10.1021/bm201176m.

[44] R. Aguado, D. Murtinho, A.J.M. Valente, Association of antioxidant monophenolic compounds with β-cyclodextrin-functionalized cellulose and starch substrates, Carbohydr. Polym. 267 (2021) 118189, https://doi.org/10.1016/j.carbpol.2021.118189.

[45] Z. Zamani, D. Alipour, H.R. Moghimi, S.A.R. Mortazavi, M. Saffary, Development and evaluation of thymol microparticles using cellulose derivatives as controlled release dosage form., Iran, J. Pharm. Res. 14 (2015) 1031–1040.

[46] S.X. Zheng, H.S. Chen, Correlations of rheological methods to coatings' performance, Prog. Org. Coat. 177 (2023) 107403, https://doi.org/10.1016/j.porgcoat.2022.107403.

[47] J.R. Varcoe, P. Atanassov, D.R. Dekel, A.M. Herring, M.A. Hickner, P.A. Kohl, A.R. Kucernak, W.E. Mustain, K. Nijmeijer, K. Scott, T. Xu, L. Zhuang, Anion-exchange membranes in electrochemical energy systems, energy, Environ. Sci. 7 (2014) 3135–3191, https://doi.org/10.1039/c4ee01303d.

[48] M. Amadu, A. Miadonye, Interrelationship of electric double layer theory and microfluidic microbial fuel cells: a review of theoretical foundations and implications for performance, Energies (Basel) 17 (2024) 1472, https://doi.org/10.3390/en17061472.

[49] K. Khwaldia, Water vapor barrier and mechanical properties of paper-sodium Caseinate and paper-sodium Caseinate-paraffin wax films, J. Food Biochem. 34 (2010) 998–1013, https://doi.org/10.1111/j.1745-4514.2010.00345.x.

[50] A. Mazega, Q. Tarrés, R. Aguado, M.À. Pèlach, P. Mutjé, P.J.T. Ferreira, M. Delgado-Aguilar, Improving the barrier properties of paper to moisture, Air, and Grease with Nanocellulose-Based Coating Suspensions, Nanomaterials 12 (2022) 3675, https://doi.org/10.3390/nano12203675.

[51] C. Tambe, D. Graiver, R. Narayan, Moisture resistance coating of packaging paper from biobased silylated soybean oil, Prog Org Coat 101 (2016) 270–278, https://doi.org/10.1016/j.porgcoat.2016.08.016.

[52] Y. Zhang, Y. Peng, R. Jia, Q. Wang, X. Lou, J. Shi, Sodium chloride combined with polypropylene film can maintain the quality of fresh-cut ginger, Food Packag. Shelf Life 25 (2020) 100541, https://doi.org/10.1016/j.fpsl.2020.100541.

[53] M.Á. López-García, Ó. López, I. Maya, J.G. Fernández-Bolaños, Complexation of hydroxytyrosol with β-cyclodextrins. An efficient photoprotection, Tetrahedron (2010), https://doi.org/10.1016/j.tet.2010.08.009.

[54] J.W.F. Law, N.S. Ab Mutalib, K.G. Chan, L.H. Lee, An insight into the isolation, enumeration, and molecular detection of Listeria monocytogenes in food, Front. Microbiol. 6 (2015) 1–15, https://doi.org/10.3389/fmicb.2015.01227.

[55] Y. Wen, J. Liu, L. Jiang, Z. Zhu, S. He, S. He, W. Shao, Development of intelligent/active food packaging film based on TEMPO-oxidized bacterial cellulose containing thymol and anthocyanin-rich purple potato extract for shelf life extension of shrimp, Food Packag. Shelf Life 29 (2021) 100709, https://doi.org/10.1016/j.fpsl.2021.100709.

[56] L. Shabala, S.H. Lee, P. Cannesson, T. Ross, Acid and NaCl limits to growth of Listeria monocytogenes and influence of sequence of inimical acid and NaCl levels on inactivation kinetics, J. Food Prot. 71 (2008) 1169–1177, https://doi.org/10.4315/0362-028X-71.6.1169.

[57] EUR-LEX, Commission Regulation No 10/2011 of January 2011 on plastic materials and articles intended to come into contact with food, Official Journal of the European Union (2011). http://data.europa.eu/eli/reg/2011/10/oj (accessed June 5, 2024).

[58] S.E. Duncan, J.B.B.T.-A. in F. and N.R. Webster, Sensory Impacts of Food–Packaging Interactions, in: M. Eskin (Ed.), Adv Food Nutr Res, Academic Press, Boston, MA, 2009: pp. 17–64. doi:https://doi.org/10.1016/S1043-4526(08)00602-5.

[59] S. Min, R. Priyadarshi, P. Ezati, J.-W. Rhim, J.T. Kim, Chitosan-based multifunctional coating combined with sulfur quantum dots to prevent Listeria contamination of enoki mushrooms, Food Packag. Shelf Life 35 (2023) 101014, https://doi.org/10.1016/j.fpsl.2022.101014.

[60] D. Rogalla, P.A. Bomar, Listeria monocytogenes, StatPearls (2023). https://www.ncbi.nlm.nih.gov/books/NBK534838/. (Accessed 5 June 2024).

[61] S. Gupta, S. Adak, R.C. Rajak, R. Banerjee, In vitro efficacy of Bryophyllum pinnatum leaf extracts as potent therapeutics, Prep. Biochem. Biotechnol. 46 (2016) 489–494, https://doi.org/10.1080/10826068.2015.1084515.

[62] S.H. Othman, N. Nordin, N.A.A. Azman, I.S.M.A. Tawakkal, R.K. Basha, Effects of nanocellulose fiber and thymol on mechanical, thermal, and barrier properties of corn starch films, Int. J. Biol. Macromol. 183 (2021) 1352–1361, https://doi.org/10.1016/j.ijbiomac.2021.05.082.

[63] P. Kranz, N. Braun, N. Schulze, B. Kunz, Sensory quality of functional beverages: bitterness perception and bitter masking of olive leaf extract fortified fruit smoothies, J. Food Sci. 75 (2010) S308–S311, https://doi.org/10.1111/j.1750-3841.2010.01698.x.

[64] P.L. Ritger, N.A. Peppas, A simple equation for description of solute release I. Fickian and non-fickian release from non-swellable devices in the form of slabs, spheres, cylinders or discs, J. Control. Release (1987), https://doi.org/10.1016/0168-3659(87)90034-4.